Marine Wastewater Discharges from Multiport Diffusers. I: Unstratified Stationary Water

Xiaodong Tian, A.M.ASCE[1]; Philip J. W. Roberts, F.ASCE[2]; and Gregory J. Daviero, A.M.ASCE[3]

Abstract: Laboratory experiments on the near-field mixing of buoyant plumes discharged from multiport diffusers into unstratified stationary water are reported. Dilution was measured by a newly developed three-dimensional laser-induced fluorescence system and a microconductivity probe. Significant additional mixing (and dilution) occurs beyond the point where the plume impacts the water surface. This mixing ceases when the turbulence generated by the plumes collapses in the surface spreading layer. The port spacing, s, was varied through a range encompassing line to point source conditions. In all cases, the concentration distribution in the surface layer eventually becomes laterally uniform. Measurements of the near-field dilution, length, and layer thickness, and semiempirical equations to predict them are presented. The discharge behaves as a line plume when $s/H \leqslant 0.3$, and as a point plume when $s/H \geqslant 1.0$. The additional near-field mixing for a point plume is much greater than for a line plume. Basing diffuser design on near-field dilution rather than impact-point dilution allows the use of far fewer ports, or risers, with considerable potential cost savings, particularly for tunneled outfalls.

DOI: 10.1061/(ASCE)0733-9429(2004)130:12(1137)

CE Database subject headings: Ocean disposal; Outfall sewers; Wastewater disposal; Model studies; Dilution; Multi-port diffuser.

Introduction

Wastewaters are frequently discharged into estuaries and coastal waters by means of outfalls and diffusers. Multiport diffusers promote rapid dilution of the effluent, reducing the concentrations of toxic and other materials and their environmental impacts to very low levels. For domestic sewage, the dilution mainly results from its buoyancy that causes it to rise as a turbulent plume, entraining ambient seawater that mixes with and dilutes the effluent. The plume stops rising when it reaches the water surface, or, if the receiving water is density stratified, a level where its density is the same as the ambient water. In either case, it then spreads horizontally, is advected by ocean currents, and diffused by oceanic turbulence.

These mixing processes are usually divided into two regions in which different physical mechanisms predominate. In the first, the mixing is intense; it results mainly from turbulence generated by the initial buoyancy and momentum of the discharge and their interactions with the ambient flow. This region is sometimes called the near field. Beyond this region, the self-induced turbulence has decayed and mixing results primarily from ambient oceanic turbulence. In this region, called the far field, dilution increases at a much slower rate than in the near field.

Other terms are used for the near field such as the hydrodynamic mixing zone and the initial dilution zone. They are often undefined or have inconsistent definitions, however. For example, Wood et al. (1993) state, "The initial dilution is that obtained by the entrainment from the surrounding fluid during the rise of the effluent from the outfall ports to its equilibrium level or the free surface. It is during this rise that the most significant portion of the dilution process occurs. It is also the only portion of the process which is under the designer's control." Further confusion can result from various definitions of *regulatory* mixing zones. For example, The Environmental Protection Agency Clean Water Act of 1977, Section 301(h) defines a zone of initial dilution (ZID) as the region of initial mixing that is the area extending a distance of one water depth from any point of the diffuser and including the water column above that area. Regulatory mixing zones, such as the ZID, have arbitrary boundaries that may or may not correspond to the predominant physical mixing processes occurring.

Significant additional mixing (and dilution) can occur beyond the location of the plume's terminal rise height. These may be caused by various processes including entrainment in the transition to horizontal flow, an internal hydraulic jump, and turbulence advected from the vertically rising plume into the horizontal layer. Here, we will use the term near field [as recommended by Doneker and Jirka (1999) and Roberts (1999)] to encompass all of these possible processes, including buoyant plume rise, surface interactions, transition to horizontal flow, and extending into some portion of the spreading layer. "Near-field processes" are therefore intimately linked to the discharge parameters and under the control of the designer. Whatever these processes are, the turbulence generated by the discharge eventually decays, and near-field mixing ceases to be significant. This marks the end of the near field, and the dilution at this point is defined as the near field dilution. In reality, the dilution asymptotically approaches its limiting value, with no sudden transition to the far field. The end of the near field is therefore considered as the location where dilution no longer changes significantly with distance; we define

[1]Postdoctoral Researcher, School of Civil and Environmental Engineering, Georgia Institute of Technology, Atlanta, Georgia, 30332.

[2]Professor, School of Civil and Environmental Engineering, Georgia Institute of Technology, Atlanta, Georgia, 30332.

[3]Malcolm Pirnie, Inc., 104 Corporate Park, Dr., White Plains, NY 10602-0751

Note. Discussion open until May 1, 2005. Separate discussions must be submitted for individual papers. To extend the closing date by one month, a written request must be filed with the ASCE Managing Editor. The manuscript for this paper was submitted for review and possible publication on August 11, 2003; approved on June 18, 2004. This paper is part of the ***Journal of Hydraulic Engineering***, Vol. 130, No. 12, December 1, 2004. ©ASCE, ISSN 0733-9429/2004/12-1137–1146/ $18.00.

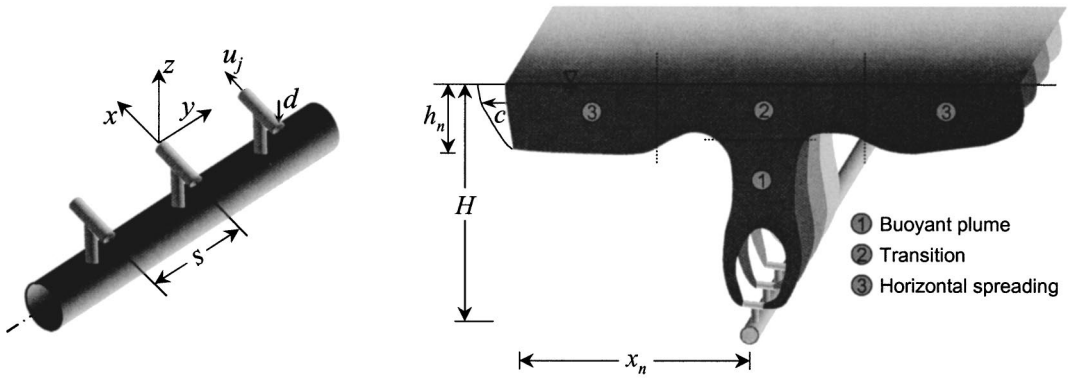

Fig. 1. Definition sketches

that as the point where the dilution is within 10% of its ultimate value.

The near-field dilution depends on the diffuser design, particularly the diffuser length and port spacing. If the ports are widely spaced, the plumes do not merge and will behave like isolated sources; if the ports are closely spaced, the plumes will merge and behave as if discharged as a line source from a slot. The dilution depends on the port spacing. Consider a diffuser where the ports are closely spaced so that the discharge behaves like a line source. If the number of ports is gradually decreased (while maintaining the diffuser length and total discharge constant so that the port spacing and flow per port increase), dilution eventually degrades (Brooks 1980) despite the decreased plume merging (contrary to some popularly held beliefs). This behavior can be seen in the model studies on the Boston outfall (Roberts and Snyder 1993). There is some controversy about the spacing where this degradation begins, however, and differing degrees of additional mixing in the spreading layer for merged and nonmerged plumes complicates the prediction of the effect of merging on dilution. Reliable prediction is needed to ensure an appropriate level of wastewater treatment and may also result in lower construction costs of ocean outfalls, particularly for tunneled outfalls with the ports contained in risers.

Most previous experiments on diffuser mixing have measured dilution from tracer concentrations obtained with point probes. Examples are Roberts et al. (1989) and Roberts and Snyder (1993). The use of point probes makes it tedious, or even impossible, to map the entire concentration field, and furthermore they cannot capture the spatial variation of instantaneous concentration fluctuations and they may disturb the flow. The advent of laser-induced fluorescence (LIF) was a major advance as it enabled the acquisition of high spatial and temporal resolution instantaneous scalar concentration fields without disturbing the flow. Most LIF studies have been planar (PLIF), however, with information obtained in two dimensions. Even relatively simple diffuser flows are inherently three dimensional (3D), however, and PLIF cannot reveal this three dimensionality.

In the present study, a newly developed three-dimensional LIF (3DLIF) system was used to investigate mixing from multiport diffusers under various conditions. Such systems have only recently become feasible due to advances in instrumentation, especially in optoelectronics, low-light high-speed cameras, high-speed scanning mirrors, image capture and processing techniques, and fast mass storage devices.

The purpose of the study was to systematically measure the effect of port spacing on near-field mixing of multiport diffusers. Experiments were conducted with various receiving environments, including stationary and flowing, stratified, and unstratified. The investigations focused on flows that are driven by buoyancy and the effects of the source momentum are negligible as this is the case most relevant to actual coastal sewage outfalls. Dilutions were measure by LIF and by a precision microconductivity probe; for further details, see Daviero (1998) and Tian (2002).

In this paper, we report the experiments in unstratified stationary water. The studies in flowing, stratified, and unstratified, waters will be presented in subsequent papers.

Analysis

The problem under consideration is sketched in Fig. 1. (The diffuser is shown with the ports contained in T-shaped risers, but the same analysis applies for ports along the diffuser side walls). The objective was to systematically examine diffuser performance over a range of port spacing from wide, resulting in individual plumes that do not merge, to narrow, resulting in plumes that fully merge. The ports are assumed to be uniformly distributed so the basic parameters are the water depth H, port diameter d, port or riser spacing s, total number of ports n, port exit velocity u_j, effluent density ρ_o, and ambient density ρ_a. Provided as the Boussinesq approximation applies, i.e., variations in fluid density are small compared to absolute densities and so are dynamically only important as buoyancy forces, the density terms can be combined as $g'_o = g(\rho_a - \rho_o)/\rho_o$, the modified acceleration due to gravity, where g is the acceleration due to gravity. The discharge can then be characterized by either point or line fluxes of volume, momentum, and buoyancy (Fischer et al. 1979) as shown in Table 1. The point and line parameters are related by

$$Q_j = \frac{Q_T}{n} \quad \text{and} \quad L = \frac{n}{2}s \tag{1}$$

where Q_T=total volume flux (flowrate) from the diffuser; and L=diffuser length.

Table 1. Discharge Fluxes from Multiport Diffusers

Variable	Point source	Line source
Volume flux	$Q_j=(\pi/4)d^2u_j$	$q=Q_T/L$
Momentum flux	$M=u_jQ_j$	$m=u_jq$
Buoyancy flux	$B=g'_0Q_j$	$b=g'_0q$

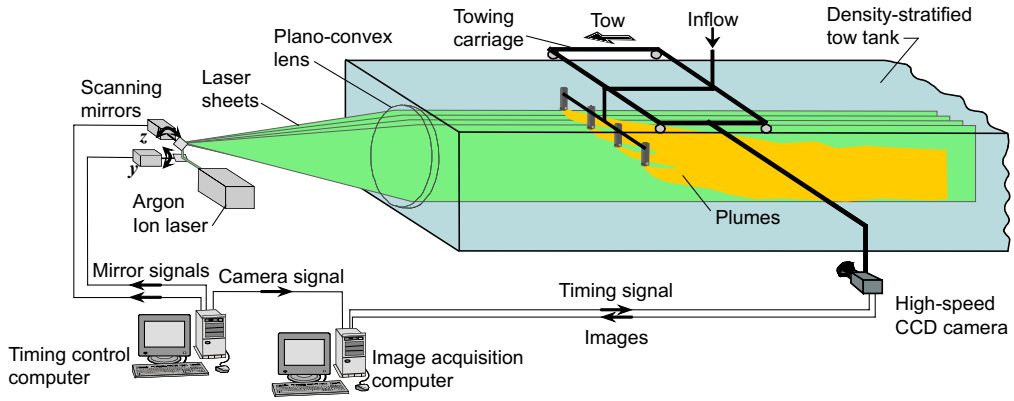

Fig. 2. Schematic depiction of three-dimensional laser-induced fluorescence system

Any dependent flow variable, ψ, can then be expressed as

$$\psi = f(B,M,s,H) \quad \text{or} \quad \psi = f(b,m,s,H) \tag{2}$$

Eq. (2) is valid as long as the dynamic effect of the source volume flux is negligible and provided the flow is fully turbulent and therefore independent of the jet Reynolds number, $\mathrm{R}=u_j d/\nu$. These are true for typical ocean outfalls and for the models tested here; this is discussed further below in the subsection entitled "Scale Effects." A dimensional analysis of Eq. (2) yields

$$\psi' = f\left(\frac{l_M}{H},\frac{s}{H}\right) \quad \text{or} \quad \psi' = f\left(\frac{l_M}{H},\frac{s}{H}\right) \tag{3}$$

where ψ'=dimensionless form of the dependent variable; and l_m and l_M=line and point source length scales that relate to the flow behavior (Fischer et al. 1979; Wright 1984; and others):

$$l_M = \frac{M^{3/4}}{B^{1/2}} \quad l_m = \frac{m}{b^{2/3}} \tag{4}$$

Many ocean sewage outfalls operate such that the flows are driven mainly by the buoyancy flux and the effect of source momentum is negligible (Roberts et al. 1989). According to Brooks (1980), this occurs when $l_M/H<0.2$ or $l_m/H<0.25$. These length scale ratios can be computed, for example, for the outfalls listed in Table 10.1 of Fischer et al. (1979), yielding: $0.02<l_M/H<0.07$ and $0.02<l_m/H<0.05$, which are clearly within the range where source momentum flux effects can be neglected. For this case, momentum can be eliminated from Eq. (2) and (3) becomes:

$$\psi' = f\left(\frac{s}{H}\right) \tag{5}$$

The wastefield characteristics of most interest here are the length of the near field, x_n, near-field dilution, S_n, and the layer thickness, h_n. The dimensionless expressions for these variables are (Daviero 1998):

$$\frac{S_n q}{b^{1/3}H} = f\left(\frac{s}{H}\right) \tag{6a}$$

$$\frac{x_n}{H} = f\left(\frac{s}{H}\right) \tag{6b}$$

$$\frac{h_n}{H} = f\left(\frac{s}{H}\right) \tag{6c}$$

Eqs. (6*a*)–(6*c*) have two limiting cases. For $s/H \ll 1$, the ports are closely spaced so that the individual discharges quickly merge and behave like a two-dimensional (2D) flow discharged from a slot. This is a "line plume" for which Eqs. (6*a*)–(6*c*) becomes:

$$\frac{S_n q}{b^{1/3}H} = C_1 \tag{7a}$$

$$\frac{x_n}{H} = C_2 \tag{7b}$$

$$\frac{h_n}{H} = C_3 \tag{7c}$$

where C_1, C_2, and C_3=experimental constants. For $s/H \gg 1$, the ports are widely spaced so that the plumes do not merge. This is a "point plume" for which the dilution is given by $S_n Q_j/B^{1/3}H^{5/3}=C_4$, where C_4 is another constant. For this case, Eqs. (6*a*)–(6*c*) become (in terms of line source variables)

$$\frac{S_n q}{b^{1/3}H} = C_7\left(\frac{s}{H}\right)^{-2/3} \tag{8a}$$

$$\frac{x_n}{H} = C_5 \tag{8b}$$

$$\frac{h_n}{H} = C_6 \tag{8c}$$

where C_5, C_6, and C_7=experimental constants and $C_7=2^{2/3}C_4$. The values of these constants were determined from the experiments and are presented below along with comparisons of values obtained by other researchers.

Experiments

Description

A schematic depiction of the experimental configuration is shown in Fig. 2. The tow tank is 6.10 m long by 0.91 m wide by 0.61 m deep. The front wall consists of two 3 m long glass panels to enable long duration tows with unobstructed views; the left wall is also glass to allow optical access for the laser. The right and rear walls and floor are steel, coated with black epoxy paint to resist corrosion and to reduce reflections. The tank is equipped

with a towing system to simulate ambient currents (not used in the present stationary experiments). The effluent, usually a mixture of fresh water, salt (NaCl), and fluorescent dye (Rhodamine 6G), is supplied from a reservoir by a rotary pump. The flow rate is measured by a precision rotameter.

The 3DLIF system is described in Tian (2002) and Tian and Roberts (2003). The beam from a continuous-wave argon-ion laser strikes two orthogonal fast galvanometer scanning mirrors that move the beam in the horizontal (y) and vertical (z) directions. The beam then strikes a large planoconvex lens and is refracted parallel to the axis of the tow tank. The laser causes the fluorescent dye to emit light that is captured by a high-speed digital charge coupled device (CCD) camera. The camera provides output in 8-bit resolution, i.e., gray scales with 256 levels, with a spatial resolution (number of active pixels) of 532 by 516. Images can be captured and streamed to hard disk at up to 260 frames per second.

The system employs two computers, one for overall timing control, and one for image acquisition. The timing control computer drives the laser beam and synchronizes it with image capture. As the beam is swept up and down once by the z mirror, the camera captures one image. The beam is then moved a small distance horizontally by the y mirror while the image is downloaded to the hard disk. This is repeated so that multiple vertical "slices" through the flow are obtained. After a predetermined number of slices, the beam returns to the starting point and the cycle starts again. For the experiments reported here, 40 slices were typically obtained at a rate of 100 frames per second. Data were obtained for about 40 s, so each experiment generated about 1 GB of data. These data were then postprocessed to extract quantitative tracer concentrations. For full details of 3DLIF system and data processing procedures, see Tian (2002) and Tian and Roberts (2003).

Separate experiments were conducted using a conductivity probe to measure dilution. The probe is a microscale conductivity and temperature sensor (Head 1983), Precision Measurement Engineering, San Diego, Model 125. It has a measuring volume of about 1.5 mm^3, and conductivity frequency response better than 500 Hz. The associated electronics provide an analog voltage output that is linearly proportional to conductivity. The signal was digitized at 12-bit resolution by a National Instruments Board, Austin, Tex., Model AT-MIO-16F-5. The probe was calibrated by immersing it in solutions containing known salt concentrations. Experiments were performed (Daviero 1998) to determine a suitable sampling frequency and duration; a sampling frequency of 30 Hz and sampling duration of 30 seconds were chosen.

Experimental Conditions

Systematic experiments were conducted to determine the effect of port spacing on near-field mixing. The tests consisted of 19 3DLIF experiments, 40 conductivity probe experiments, and 12 PLIF experiments to determine spreading layer thickness only. The model diffuser consisted of T-shaped risers each with two ports 3.2 mm diameter. The number of risers varied from 1 to 17 and the ports were submerged 25.4 mm beneath the water surface. The parameter range investigated was $0.1 < s/H < 4.9$, $1.4 < H/l_M < 42.9$, and $1.7 < H/l_m < 29.3$. Most experiments were in the buoyancy dominated region ($H/l_M > 5$ and $H/l_m > 4$), as this is the case most relevant to ocean sewage outfalls. For summaries of the 3DLIF experiments, see Tian (2002), Table 5.1, and for the conductivity probes experiments, see Daviero (1998), Tables 4.1 and 4.2.

The end of the near field is the location where dilution no longer changes significantly with distance from the diffuser. This was defined as where the dilution is within 10% of its ultimate value. Dilutions were measured by the conductivity probe and 3DLIF. For an unstratified environment, the minimum dilution and upper layer boundary are always at the water surface. The layer thickness, h_n, was determined from the LIF images with the lower boundary defined as where the tracer concentration is 10% of the maximum (surface) value.

Scale Effects

The scaling laws, Eq. (3), do not preserve the similarity of the source volume flux or jet Reynolds number between the model and prototype. The consequences of this are discussed below.

The relative importance of source volume flux can be quantified by the length scales $l_Q = Q/M^{1/2}$ (for a point source) and $l_q = q^2/m$ (for a line source). The significance of these length scales has been discussed in many publications, including Brooks (1980) and Wright et al. (1982). If $l_Q/H \ll 1$ and $l_q/H \ll 1$, then the source volume flux has little dynamic effect on the flow. These requirements can be expressed in terms of the port geometry. For a point source, $l_Q = d\sqrt{\pi/4}$, and for a line source, $l_q = w$, the width of an equivalent slot. Therefore, $l_Q/H \ll 1$ is equivalent to $d/H \ll 1$, and $l_q/H \ll 1$ is equivalent to $w/H \ll 1$, i.e., the source geometry does not affect the flow. Again, typical values of these ratios can be obtained for the outfalls listed in Table 10.1 of Fischer et al. (1979), yielding $0.001 < d/H < 0.003$, and $0.0001 < w/H < 0.001$. Clearly, the nozzle size is not a relevant scale for typical outfalls, so volume flux effects can be neglected. This is also true for all the experiments here.

The Reynolds numbers in the model are much smaller than in prototype outfalls. In contrast to flows with solid boundary effects, however, free-shear flows, such as the jets and plumes studied here, are not strongly dependent on the value of Reynolds number, provided they are turbulent. This has been discussed by Snyder (1981), Isaacson et al. (1983), Roberts et al. (1989), and Roberts and Snyder (1993). The consequences of low model Reynolds numbers are reduced entrainment near the nozzles and a slightly increased rise height of the receiving water is stratified, i.e., measured dilutions will tend to be conservatively low compared to the prototype. Results quoted by Snyder suggest that buoyant plume rise from vertical stacks is independent of Reynolds numbers for $R > 300$. Roberts and Snyder (1993) observed, as did Isaacson et al. (1983) and Roberts et al. (1989), that, even if the plumes are initially laminar, they become turbulent soon after entering the tank. Roberts et al. (1989) ran specific tests to study the effect of Reynolds number and found none for $R = 450$, 1,070, and 1,480.

The above assumptions have recently received strong substantiation from comparisons of the results of field tests on the Boston outfall with 3DLIF laboratory measurements that were made to recreate the observed field conditions (Roberts et al. 2002). The field and laboratory measurements of dilution and wastefield thickness were in excellent agreement, confirming that the small-scale experiments can be scaled up to prototype conditions.

Experimental Results

Three-Dimensional Visualizations

Volume rendering was used to visualize the huge amounts of LIF data obtained. Top and bottom perspective views of the flow cre-

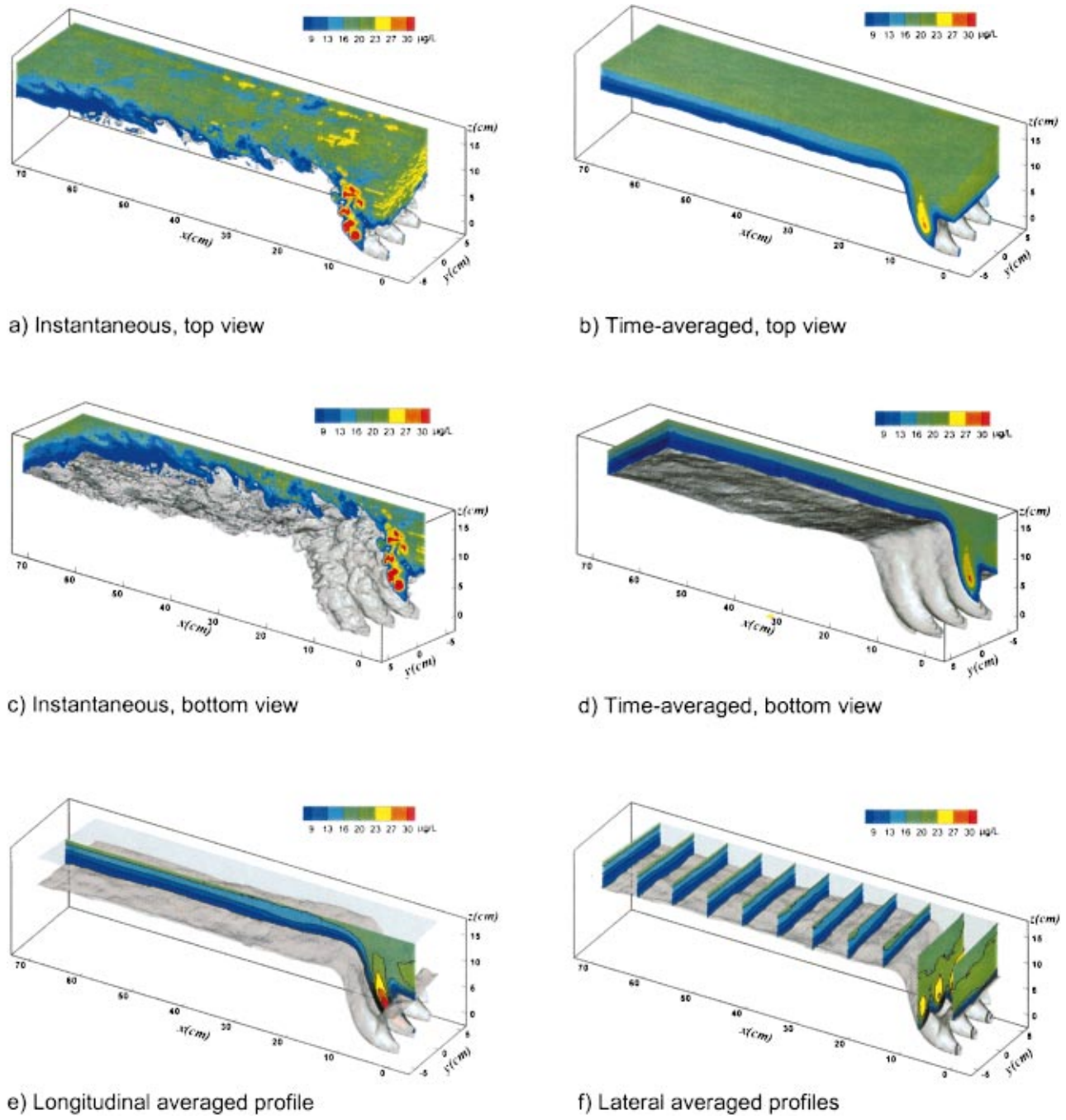

Fig. 3. (Color) Flow from closely spaced ports ($s/H=0.21, c_o=800$ μg/L)

ated by a diffuser with closely spaced ports are shown in Fig. 3. Figs. 3(a–d) show instantaneous and time-averaged top and bottom views. The outer plume surfaces are shown in gray by generating an isosurface of a concentration level just above zero. Local concentrations, c, are displayed in vertical and horizontal planes as pseudocolors keyed to concentration levels. The local dilution can be obtained from these figures as $S=c_o/c$, where c_o is the source dye concentration. To increase the spatial resolution, only one side of the diffuser and only 3 of the 17 risers in this test were captured.

A great benefit of 3DLIF is the ability to capture instantaneous flow characteristics. The visualizations of instantaneous fields [Figs. 3(a and c)], show patchy concentration distributions with large variations in magnitude, especially close to the diffuser. The outer surface of the spreading layer is wrinkled and folded, indicating the presence of vortices. These vortices cause additional mixing as discussed later. In the time-averaged visualizations [Figs. 3(b and d)], the spatial variations of concentration and the outer isosurface are smooth.

Time-averaged concentration profiles in longitudinal and lateral vertical planes are shown in Figs. 3(e and f)). Here, the outer isosurface and the water surface (the horizontal top plane) are made semitransparent to reveal the inner concentration distribution. Fig. 3(e) shows a longitudinal profile along a port centerline. There appears to be a slight increase in layer thickness just after the plume impacts the water surface which may be an internal hydraulic jump.

The spatial variability in these concentration profiles is better

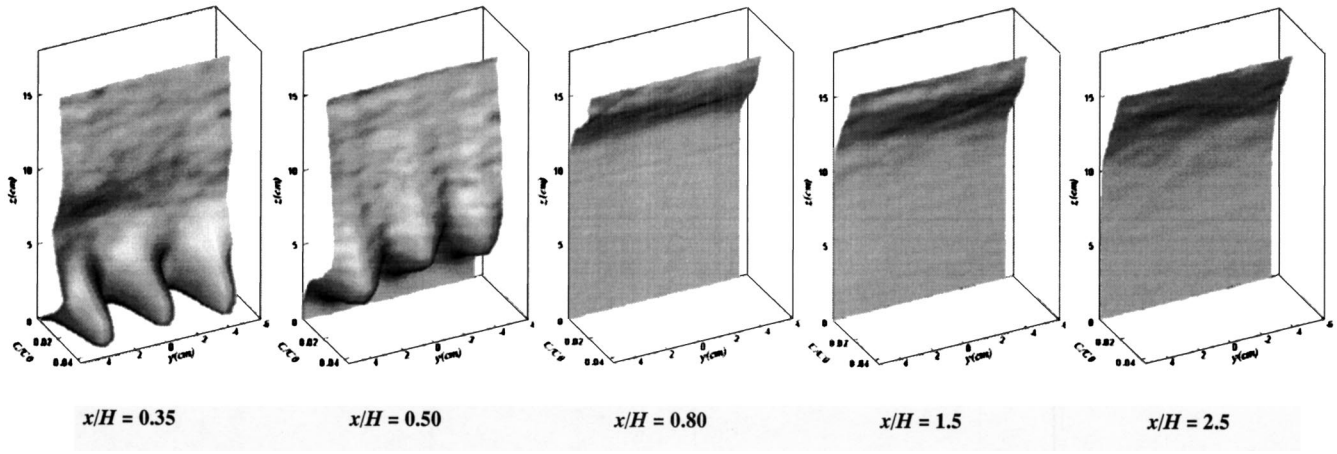

Fig. 4. Lateral concentration profiles for closely spaced ports ($s/H=0.21$)

shown by 3D surface relief plots, Fig. 4. These are lateral profiles at various distances from the diffuser [same as Fig. 3(f)] where the height of the relief is the normalized tracer concentration, c/c_o. The plume merging can be clearly seen; for this case, they begin to merge before reaching the water surface. Close to the diffuser, at $x/H=0.35$, the three individual plumes have not merged and are quite distinct. They are partially merged at $x/H=0.5$, near where they impact the water surface. Beyond this point, lateral mixing is rapid so that by $x/H\approx 0.8$, no evidence of the individual plumes remains and the profiles are laterally uniform.

Similar behavior was observed in studies of San Francisco outfall (Isaacson et al. 1983), and the experiments of Roberts et al. (1989) and Roberts and Snyder (1993). In these studies, however, each lateral profile had only 100 sampling points or fewer, and repeated experiments were needed to obtain each profile. Far more data can be obtained with the 3DLIF system. For the experiment above, each CCD image had approximately 74,2000 (530×140) data points, and 40 planes were imaged. Figs. 3 and 4 therefore represent almost 3 million sampling points, vastly more than can be obtained by point sampling methods. The profiles are therefore much more detailed and show the lateral structures more clearly. (An animation is also available that shows a lateral profile moving from $x=0$ through the area imaged.)

Similar results for widely spaced ports are shown in Figs. 5 and 6. (For this example, the effect of momentum was not negligible, although the following observations also apply to the plume case). Only one of the three risers in this test is shown and the images begin 14 cm from the diffuser. The increased layer thickness beyond the surface impact point suggests the presence of an internal hydraulic jump. The plumes do not interfere before reaching the water surface [Figs. 5(d) and 6]. Beyond this point, they merge and spread laterally so that the profiles again eventually become laterally uniform, despite the very wide port spacing for this case. The profiles are fully merged at $x/H\approx 7.0$ and beyond. This distance is much longer than that for the closely spaced ports.

Dilution

The variation of minimum dilution with distance from the diffuser was computed for all experiments. As previously discussed, dilution approaches its ultimate value asymptotically, and the end of the near field was defined as the location where the dilution was within 10% of its ultimate value. The near-field dilutions were obtained in this way and are plotted in normalized form [Eq. (6)] in Fig. 7. For $s/H<0.3$, the results follow the line plume Eq. (7*a*). A best fit to the data yields $C_1=0.49$, so Eq. (7*a*) becomes

$$\frac{S_n q}{b^{1/3}H}=0.49 \tag{9}$$

For $s/H>0.3$, the results begin to deviate from a line plume and normalized dilution decreases. For $s/H\geqslant 1.0$, the results follow the point plume Eq. (8*a*) and a best fit to the data yields $C_7=0.41$ so Eq. (8*a*) becomes:

$$\frac{S_n q}{b^{1/3}H}=0.41\left(\frac{s}{H}\right)^{-2/3} \tag{10a}$$

or

$$\frac{S_n Q_j}{B^{1/3}H^{5/3}}=0.26 \tag{10b}$$

Similarly, the variations of near-field length, x_n, and spreading layer thickness, h_n, with riser spacing are shown in Figs. 8 and 9. For line plume conditions [Eqs. (7*b*) and (7*c*)], best fits to the data yield $C_2=0.90$ and $C_3=0.36$, so Eqs. (7*b*) and (7*c*) become

$$\frac{x_n}{H}=0.90 \tag{11a}$$

and

$$\frac{h_n}{H}=0.36 \tag{11b}$$

For point plume conditions [Eqs. (8*b*) and (8*c*)], best fits to the data yield $C_5=2.8$ and $C_6=0.11$, so Eqs. (8*b*) and (8*c*) become

$$\frac{x_n}{H}=2.8 \tag{12a}$$

and

$$\frac{h_n}{H}=0.11 \tag{12b}$$

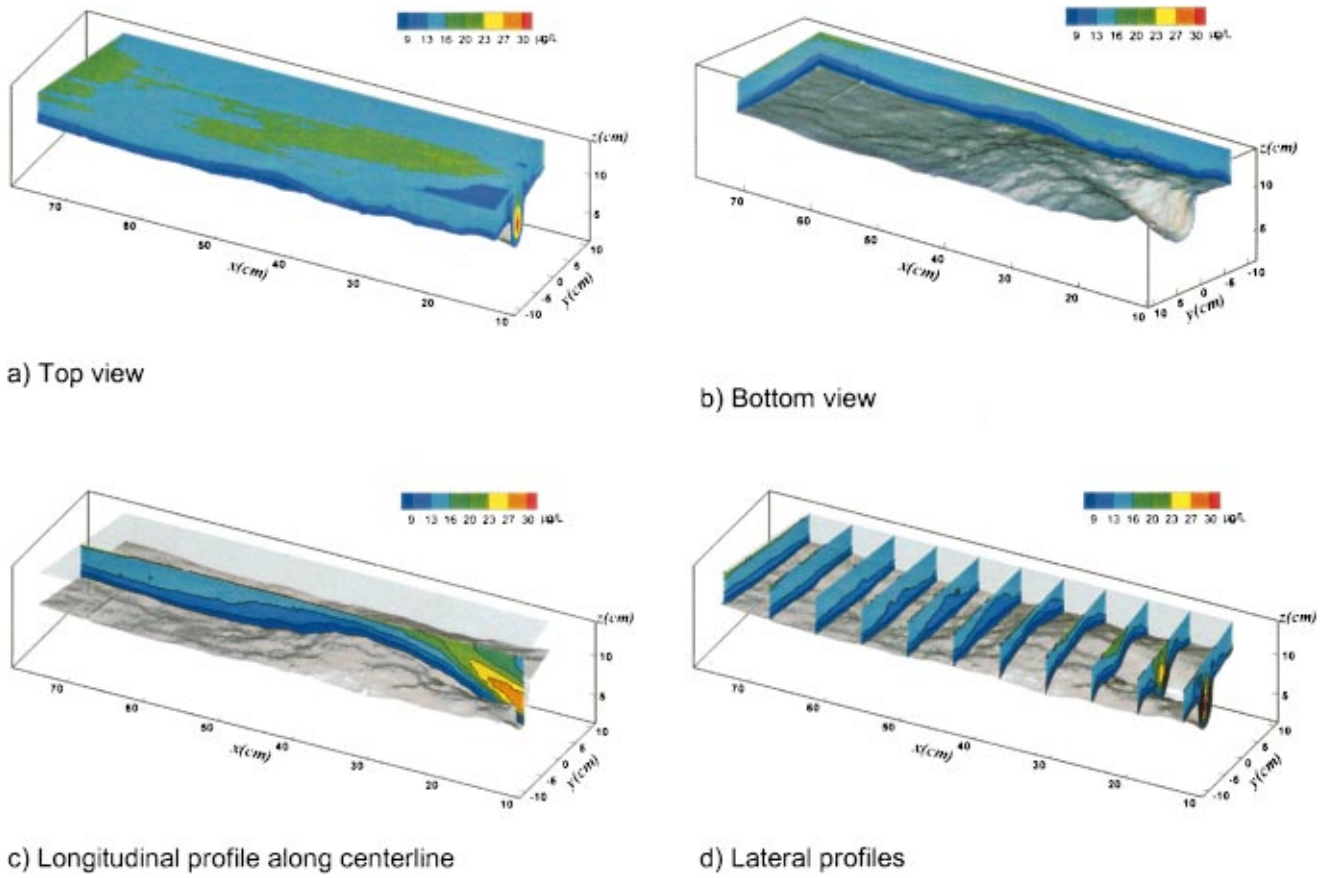

Fig. 5. (Color) Flow from widely spaced ports ($s/H=4.0, c_o=500$ μg/L)

Discussion

The near-field dilution can be predicted by the line plume Eq. (9) when $s/H \leq 0.3$, and by the point plume Eqs. (10*a*) and (10*b*) when $s/H \geq 1$. Previous researchers have reported different values of the constants in these equations depending on the diffuser geometry and the location of the dilution measurement. For a line plume, the measured coefficient, C_1 [Eq. (9)] is 0.49. Rouse et al. (1952) and Kotsovinos (1975) measured centerline dilutions in a freely rising line plume and obtained $C_1=0.42$. Koh and Brooks (1975) performed a theoretical entrainment analysis of a line plume in finite water depth. They assumed that the presence of the surface layer reduced dilution (contrary to the present findings) and estimated $C_1=0.38$. For a point plume, the measured coefficient [Eq. (10*b*)], C_4 is 0.26. Rouse et al. (1952) measured the centerline dilution of a freely rising point plume and obtained $C_4=0.091$.

These coefficients reported by other researchers are lower than obtained here because they do not include the additional mixing that occurs within the spreading layer. The coefficients reported here [Eqs. (9) and (10)] include all of these additional near-field mixing processes. Note also that the present coefficients are derived for configurations more typical of actual outfalls with ports discharging from both sides of the diffuser. This should result in coefficients somewhat higher than for a discharge from a single slot due to the additional entrainment at the inside faces of the horizontally opposed plumes.

The magnitude of the additional dilution that occurs in the

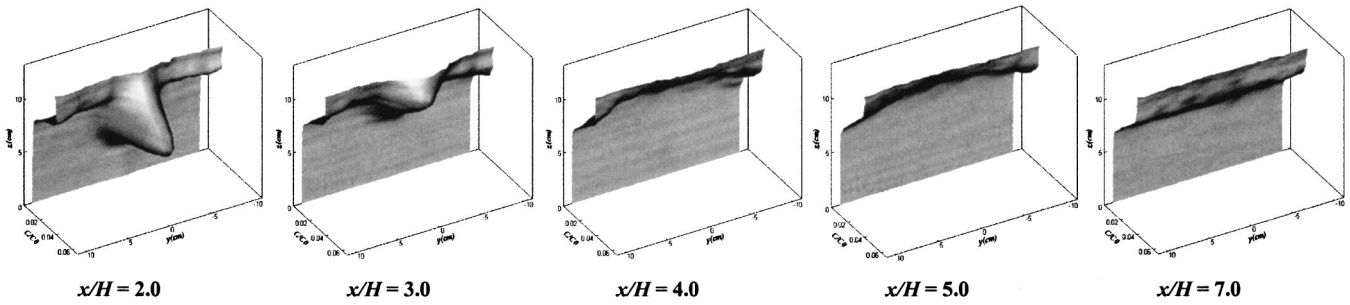

Fig. 6. Lateral concentration profiles for widely spaced ports ($s/H=4.0$)

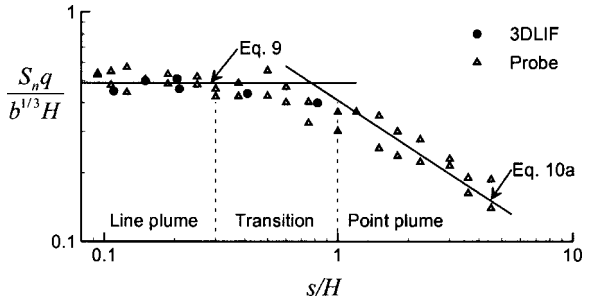

Fig. 7. Variation of near-field dilution with riser spacing

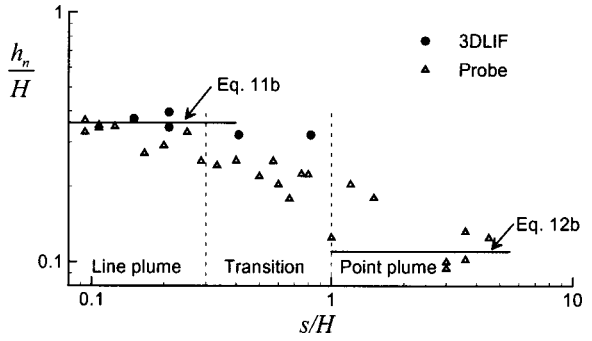

Fig. 9. Variation of spreading layer thickness with riser spacing

spreading layer can be estimated by comparing the values of the coefficients applicable to the near field to those at the centerline of a freely rising plume. For a line plume, the near-field coefficient is 0.49, whereas the coefficient for centerline dilution (Rouse et al. 1952) is 0.42. Therefore, the ratio of near-field dilution to centerline dilution is $0.49/0.42 \approx 1.2$, indicating a 20% increase in dilution for line plumes. Similarly, for a point plume, the ratio is $0.26/0.091 \approx 3$, indicating a 200% increase in dilution for point plumes. These values are reasonably consistent with findings of other researchers. For a line plume, Wood et al. (1993) predicted the dilution to increase by a factor of about 1.3 and Wright (1984) estimated an increase in average dilution of about 1.12. For a point plume, Wood et al. (1993) predicted the dilution to increase by a factor of about 2, Wright et al. (1991) estimated an increase in dilution by a factor of about 3, and Woodson and Tian (1999) directly measured centerline and near-field dilutions and estimated the dilution to increase by a factor of 3.1. It is clear that the increase in dilution of a point plume after impact with the water surface is much greater than that for a line plume.

Investigations to explain the reasons for this difference and the nature of the mixing processes in the spreading layer are reported in Daviero (1998). He observed that rolling vortices are generated at the impact point that propagate away and subsequently collapse. These vortices appear to be efficient entrainment mechanisms. There are two fundamental differences between a point and a line plume. The spreading layer of a point plume is relatively thin [0.11*H*, Eq. (12*b*)] and is 3D, whereas the spreading layer from a line plume is considerably thicker [0.36*H*, Eq. (11*a*)] and 2D.

Vortices resulting from a point plume are shown in Daviero (1998) (his figures 5.3 and 5.4). They are periodic "ring" structures originating where the plume impacts the water surface. The concentration fluctuations there are large with substantial high-frequency content. The size of the vortices is approximately the same as the layer thickness and they extend over the entire spreading layer. They propagate away radially and entrain ambient fluid which can extend all the way to the water surface (as indicated by concentration fluctuations measured at various radial distances). The vortices slow as they travel so that each subsequent vortex gains on the previous one until they coalesce and ultimately break down. Similar observations were noted by Wright et al. (1991) and Alavian and Hoopes (1982) in their investigation of thermal fronts in heated water discharges, and Linden and Simpson (1994) in a study of dense gas dispersion.

Mixing continues beyond the point where these vortices coalesce, and Roberts et al. (1997) discussed possible mixing processes occurring in this region. Initially, it is presumably caused by turbulence originating in the rising plume and the vortices. Farther away, it probably changes to a gravitational diffusion process similar to that analyzed by Rouse (1947) whereby the heavier fluid elements sink and the lighter fluid elements rise. This creates a stable density profile that ultimately causes the turbulence generated in the near field to collapse and mixing to cease. Because of the complexity of the turbulence energetics in this region, no analysis was attempted, although the observations of turbulence collapse of Ivey and Imberger (1991), used Roberts et al. (1997) may be applicable. Regardless of the mechanism, Daviero (1988) (his figure 5.4) demonstrates that most high-frequency turbulent fluctuations have ceased at three water depths from the source.

Vortices resulting from a line plume are shown in Daviero (1998) (his figures 5.5 and 5.6). They also originate where the plume impacts the water surface. The concentration fluctuations again have a substantial high-frequency component but their amplitudes are smaller than those for a point plume. The vortices typically occupy about one-third of the spreading layer thickness; concentration time series indicate that no additional ambient fluid is transported all the way to the water surface. The vortices slowly move into the thicker horizontal spreading layer and quickly break down, entraining less ambient fluid. Beyond this region, the turbulent fluctuations rapidly decay under the influence of the stable density field in a manner similar to that discussed above for point plumes.

These observations help explain the difference in the near-field lengths for point and line plumes. The end of the near field occurs at about 0.9*H* [Eq. (11*a*)] for a line plume and about 2.8*H* [Eq. (12*a*)] for a point plume. No other measurements of near-field length for line plumes are known; the value for a point plume is somewhat smaller than the approximately 3 to 5 water depths estimated by Wright et al. (1991).

The wastefield thickness is much greater for a line plume than for a point plume. For a line plume it is about 0.36*H* [Eq. (11*b*)]

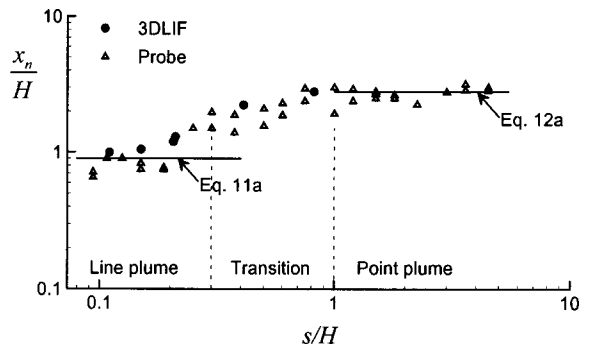

Fig. 8. Variation of near-field length with riser spacing

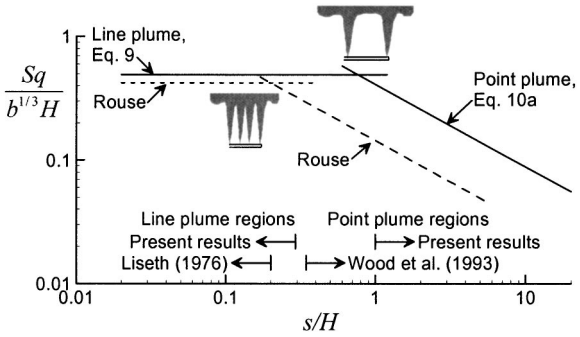

Fig. 10. Design criteria for multiport diffusers

and for a point plume about $0.11H$ [Eq. (12*b*)]. The line plume result is similar to that presented by previous researchers. Liseth (1976) and Roberts (1979) reported a thickness of $0.3H$ and Bühler (1974) reported $0.4H$ based on experimental measurements, while Koh and Brooks (1975) predicted a wastefield thickness of $0.3H$ based on a theoretical analysis. The point plume result is smaller than the $0.16H$ value measured by Wright et al. (1991).

Practical Implications

The limits of applicability of the line and point plume equations inferred from Fig. 7 differ from those suggested by other researchers. The line plume equation applies for $s/H<0.3$, whereas Liseth's (1976) measurements in the freely rising plume indicated that the discharge behaves as a line plume for $s/H<0.2$. Similarly, the point plume equation applies for $s/H>1$, whereas Wood et al. (1993) suggest that if $s/H>0.33$ there is no plume interference and the point plume formula applies. The limits proposed by Liseth and Wood et al. are smaller than those reported here because they do not consider the additional dilution in the spreading layer and, particularly, the different increase in dilution between point and line plumes.

This is illustrated in Fig. 10. The line plume Eq. (9) is a horizontal line, and the point plume Eq. (10*a*) is a line of slope $-2/3$. The intersection of these two straight lines is roughly the division between line and point plumes. When the measured near-field dilution constants are used [Eqs. (9) and (10*a*)], the intersection occurs at $s/H\approx 0.8$. If the coefficients for freely rising plumes from Rouse et al. (1952) ($C_1=0.42$ and $C_4=0.091$ or $C_7=0.14$) are used, the intersection point shifts to $s/H\approx 0.2$. The shift is because of the much greater additional dilution that occurs for point plumes than for line plumes.

This observation has considerable practical significance. For a fixed diffuser length, dilution is maximized when the ports are closely spaced and approximate a line plume. Decreasing the number of ports, therefore increasing their spacing, causes dilution to degrade. To illustrate this, assume that the "design point," where dilution begins to degrade, is where the line and point plume equations intersect. If the diffuser design is based on near-field dilution, the ports would be spaced about 0.8 water depths apart. If based on impact point centerline dilution, the diffuser would be about 20% longer with ports spaced about 0.2 water depths apart, i.e., more than four times as many ports would be needed. This is particularly important when the ports are contained in costly risers, such as the tunneled Boston outfall. It also helps to explain some of the physical model results that Roberts and Snyder (1993) observed for that outfall. There was little effect on dilution as the number of risers was increased (with the diffuser length fixed) beyond 55, with a riser spacing of 37.2 m. The risers each contained eight ports, and the plume rise height was about 20 m, so the ratio of port spacing to rise height (if contained in T-shaped risers as defined here) would be $s/H\approx 0.5$. This is roughly consistent with the recommendations given above, but is a much wider spacing (with far fewer risers) than if the recommendations of Wood et al. (1993) or Liseth (1976) were followed.

Conclusions

Experiments on the near-field mixing of wastewaters discharged from multiport diffusers are presented. In this paper, results in unstratified stationary water are discussed. Dilutions were measured by a newly developed 3DLIF and a microconductivity probe. Both instantaneous and time-averaged 3D images of these flows were constructed that clearly show the spatial concentration distributions.

Significant additional mixing (and dilution) occurs beyond the point where the plume impacts the water surface. This additional mixing is caused by various processes, possibly including entrainment in the horizontal flow transition, an internal hydraulic jump, and by turbulence advected from the vertically rising plume into the horizontally spreading layer. The term near field is used to encompass all of these possible mixing processes, which are therefore intimately linked to the discharge parameters. The end of the near field is defined as the point where dilution no longer changes significantly with distance from the diffuser. This is presumably where the turbulence generated in the near field collapses under the influence of the stably stratified spreading layer.

The port spacing was varied through a range encompassing line plume to point plume conditions. For line plume conditions, the individual plumes begin to merge before impacting the water surface. The concentration distribution then quickly becomes laterally uniform as the plumes fully merge in the surface spreading layer. For point plume conditions, the plumes did not merge before the impact point, but did merge afterward, again ultimately leading to a laterally well-mixed wastefield.

The near-field characteristics of most interest to outfall design and prediction are reported. These are the dilution, near-field length, and spreading layer thickness; semiempirical equations to predict them are presented [Eqs. (9) and (12)]. A discharge into an unstratified sationary environment behaves as a line plume when $s/H\leqslant 0.3$ and like a point plume when $s/H\geqslant 1.0$. The additional mixing in the spreading layer for a point plume is much greater than for a line plume. If diffuser design is based on near-field dilution, rather than impact-point dilution, far fewer ports, or risers, can be used with considerable potential cost savings.

Acknowledgments

The writers acknowledge the support of the National Science Foundation under Grant Nos. DGE-9354986 and CBT-8915537 and the STAR program of the U.S. Environmental Protection Agency, Exploratory Research, Physics, Grant Number R826216. Ms. Karen Maile is also thanked for her help in conducting the conductivity probe experiments.

Notation

The following symbols are used in this paper:

B = point-source buoyancy flux;
b = line-source buoyancy flux;
$C_{1\ldots7}$ = experimental constants;
c = local tracer concentration;
c_0 = source tracer concentration in the outfall pipe;
d = port diameter;
g = acceleration due to gravity;
H = water depth;
h_n = thickness of wastefield at end of near field;
L = diffuser length;
l_M = point-source length scale;
l_m = line-source length scale;
M = point-source momentum flux;
m = line-source momentum flux;
n = total number or ports;
R = jet Reynolds number;
S = dilution;
S_n = near-field dilution;
s = port spacing;
Q_T = total flow rate;
Q_j = flow rate per port;
q = flow rate per unit diffuser length;
u_j = port exit velocity;
w = equivalent slot jet width for a line source;
x_n = length of near field;
ρ_a = ambient density at level of ports;
ρ_o = effluent density;
ν = kinematic viscosity; and
ψ, ψ' = arbitrary variables.

References

Alavian, V., and Hoopes, J. A. (1982). "Thermal fronts in heated water discharges." *J. Hydraul. Div., Am. Soc. Civ. Eng.*, 108(5), 707–725.

Brooks, N. H. (1980). "Synthesis of stratified slow phenomena for design of outfalls." *Proc., 2nd Int. Symp. on Stratified Flows*, Trondheim, Norway, 809–831.

Bühler. (1974). "Model studies of multiport outfalls in unstratified, stagnant or flowing receiving waters." PhD thesis, Dept. of Civil Engineering, University of California, Berkeley, Calif.

Daviero, G. (1998). "Hydrodynamics of ocean outfall discharges in unstratified and stratified flows." PhD thesis, School of Civil Engineering, Georgia Institute of Technology, Atlanta.

Doneker, R. L., and Jirka, G. H. (1999). "Discussion of mixing of inclined dense jets' by Roberts, P. J. W., Ferrier, A., and Daviero, G." (1997)." *J. Hydraul. Eng.*, 125(3), 317–319.

Fischer, H. B., List, J. E., Koh, R. C. Y., Imberger, J., and Brooks, N. H. (1979). *Mixing in inland and coastal waters*, Academic, San Diego.

Head, M. J. (1983). "The use of miniature four-electrode conductivity probes for high-resolution measurement of turbulent density or temperature variations in salt-stratified water flows." PhD thesis, Univ. of California, San Diego.

Isaacson, M. S., Koh, R. C. Y., and Brooks, N. H. (1983). "Plume dilution for diffusers with multiple risers." *J. Hydraul. Eng.*, 109(2), 199–220.

Ivey, G. N., and Imberger, J. (1991). "On the nature of turbulence in a stratified fluid. I: Energetics of mixing." *J. Phys. Oceanogr.*, 21(5), 650–658.

Koh, R. C. Y., and Brooks, N. H. (1975). "Fluid mechanics of wastewater disposal in the ocean." *Annu. Rev. Fluid Mech.*, 7, 187–211.

Kotsovinos, N. E. (1975). "A study of the entrainment and turbulence in a plane buoyant jet." PhD thesis, California Institute of Technology, Pasadena, Calif.

Linden, P. F., and Simpson, J. E. (1994). "Continuous releases of dense fluid from an elevated point source in a cross-flow." *Mixing and transport in the environment*, K. J. Beven, P. C. Chatwin, and J. H. Millbank, eds., Wiley, New York, 401–418.

Liseth, P. (1976). "Wastewater disposal by submerged manifold." *J. Hydraul. Div., Am. Soc. Civ. Eng.*, 102(1), 1–14.

Roberts, P. J. W. (1979). "Line plume and ocean outfall dispersion." *J. Hydraul. Div., Am. Soc. Civ. Eng.*, 105(4), 313–331.

Roberts, P. J. W. (1999). "Closure to mixing in inclined dense jets." (1997). *J. Hydraul. Eng.*, 125(3), 318–319.

Roberts, P. J. W., Snyder, W. H., and Baumgartner, D. J. (1989). "Ocean outfalls I. submerged wastefield formation." *J. Hydraul. Eng.*, 115(1), 1–25.

Roberts, P. J. W., and Synder, W. H. (1993). "Hydraulic model study for the Boston outfall. I: Riser configuration." *J. Hydraul. Eng.*, 119(9), 970–987.

Roberts, P. J. W., Ferrier, A., and Daviero, G. (1997). "Mixing in inclined dense jets." *J. Hydraul. Eng.*, 123(8), 693–699.

Roberts, P. J. W., Hunt, C. D., and Mickelson, M. J. (2002). "Field and model studies of the Boston outfall." *Proc., 2nd Int. Conf. on Marine Waste Water Discharges*, MWWD2002, Istanbul, Turkey.

Rouse, H. (1947). "Gravitational diffusion from a boundary source in two-dimensional flow." *ASME J. Appl. Mech.*, A225–A228.

Rouse, H., Yih, C. S., and Humphreys, H. W. (1952). "Gravitational convection from a boundary source." *Tellus*, 4, 201–210.

Synder. (1981). "Guideline for fluid modeling of atmospheric dispersion." *Rep. No. EPA-600/S/81/009*, U.S. Environmental Protection Agency, Research Triangle Park, N.C.

Tian, X. (2002). "3DLIF and its applications to studies of the near-field mixing of wastewater discharge." PhD thesis, School of Civil and Environmental Engineering, Georgia Institute of Technology, Atlanta.

Tian, X., and Roberts, P. J. W. (2003). "A 3DLIF system for turbulent buoyant jet flows." *Exp. Fluids*, 35, 636–647.

Wood, I. R., Bell, R. G., and Wilkinson, D. L. (1993). "Ocean disposal of wastewater." World Scientific, Singapore.

Woodson, C. B., and Tian, X. (1999). "Investigation of mixing dynamics in a surfacing buoyant plume." School of Civil Engineering, Georgia Institute of Technology, Atlanta.

Wright, S. J. (1984). "Buyoant jets in density-stratified crossflow." *J. Hydraul. Eng.*, 110(5), 643–656.

Wright, S. J., Wong, D. R., Zimmerman, K. E., and Wallace, R. B. (1982). "Outfall diffuser behavior in stratified ambient fluid." *J. Hydraul. Div., Am. Soc. Civ. Eng.*, 108(4), 483–501.

Wright, S. J., Roberts, P. J. W., Zhongmin, Y., and Bradley, N. E. (1991). "Surface dilution of round submerged buoyant jets." *J. Hydraul. Res.*, 29(1), 67–89.